How Interphase Properties Control the Young's Modulus and Yield Strength of Polymer Nanocomposites?

Y. Zare[1] and K.-Y. Rhee[2]*

[1] *Biomaterials and Tissue Engineering Research Group, Department of Interdisciplinary Technologies,*
Breast Cancer Research Center, Motamed Cancer Institute, ACECR, Tehran, 14155-4364 Iran
[2] *Department of Mechanical Engineering, College of Engineering, Kyung Hee University,*
Yongin, 446-701 Republic of Korea
* e-mail: rheeky@khu.ac.kr

Abstract—In this article, several models are applied to reveal the effects of volume fraction, thickness, strength and modulus of interphase region between polymer matrix and nanofiller on the Young's modulus and yield strength of polymer nanocomposites. The properties of interphase are calculated for several samples by experimental data of mechanical properties. It is found that the concentration of interphase is higher than that of nanofiller in some samples. The Young's modulus of nanocomposites largely depends on filler and interphase concentrations. In addition, the highest fraction and strength of interphase region produce the highest yield strength of nanocomposites.

Keywords: polymer nanocomposites, interphase properties, mechanical behavior, micromechanics models

1. INTRODUCTION

Nanostructures suggest novel applications due to the excellent properties of materials at nanoscale [1–4]. Therefore, the structure and interaction at nanoscale cause the significant effects on the properties. The dramatic enhancement in the mechanical properties of polymers can be attained by incorporation of a low weight percentage (wt %) of various nanofillers such as layered silicates [5, 6]. The large aspect ratio and stiffness of layered silicates may be the main reasons for the highly enhanced mechanical properties of polymer nanocomposites [7].

The Young's modulus of polymer nanocomposites increases by addition of nanoparticles, because they usually have a much higher modulus than polymer matrices [8–10]. However, the yield strength of nanocomposites depends on the stress transferal between nanofiller and polymer matrix [11]. The stress applied to nanocomposites can be excellently transferred to nanoparticles in well-bonded nanoparticles to polymer matrix. In this condition, the yield strength of polymer nanocomposites noticeably improves in the tensile test. However, the yield strength reduces by adding of poorly bonded nanoparticles. As a result, the proper-

ties of interface/interphase between polymer matrix and nanoparticles cause main effects on the mechanical properties of polymer nanocomposites and discounting of interphase characteristics results in wrong prediction of nanocomposites performances [12, 13].

The interphase dimension and stiffness have been determined by micromechanical models for mechanical behavior such as Young's modulus and tensile/yield strength [14, 15]. It was also reported that shape memory polymer nanocomposites with a strong adhesion at polymer–nanofiller interface show pronounced shape memory properties [16]. However, there is not a model which directly expresses the effects of interphase properties such as interphase fraction on the Young's modulus and yield strength.

In this work, Ji and Pukanszky models are used to display the Young's modulus and yield strength of polymer nanocomposites containing different filler geometries as a function of the volume fraction, thickness, tensile strength and modulus of interphase region. The influences of interphase properties on the Young's modulus and yield strength of nanocomposites are discussed. Additionally, the mentioned equations are used to analyze the properties of interphase in various samples.

2. BACKGROUND

Ji et al. [17] proposed a three-phase model for Young's modulus of nanocomposites taking into account matrix, nanofiller and interphase between polymer and nanoparticles. The Ji model for nanocomposites containing layered (1), spherical (2) and cylindrical (3) nanoparticles is expressed attributed to geometry of nanofillers as

$$E = E_m \left(1 - \alpha + \frac{\alpha - \beta}{1 - \alpha + \alpha(k-1)/\ln k} \right.$$
$$\left. + \frac{\beta}{1 - \alpha + 1/2(\alpha - \beta)(k+1) + \beta E_f/E_m} \right)^{-1}, \quad (1)$$

$$\alpha_1 = \sqrt{(2t_i/t + 1)\varphi_{f1}}, \quad (2)$$

$$\alpha_2 = \sqrt{(r_{i2}/r_2 + 1)^3 \varphi_{f2}}, \quad (3)$$

$$\alpha_3 = \sqrt{(r_{i3}/r_3 + 1)^2 \varphi_{f3}}, \quad (4)$$

$$\beta = \sqrt{\varphi_f}, \quad (5)$$

$$k = \frac{E_i}{E_m}, \quad (6)$$

where E_m, E_f and E_i are the Young's moduli of matrix, nanofiller and interphase, respectively, φ_f is volume fraction of nanofiller, r and t are the radius and thickness of nanofillers, respectively, and r_i and t_i are the thickness of interphase.

The volume fractions of interphase φ_i in different polymer nanocomposites are defined as

$$\varphi_{i1} = \varphi_{f1} 2t_i/t, \quad (7)$$

$$\varphi_{i2} = \varphi_{f2}[((r_2 + r_{i2})/r_2)^3 - 1], \quad (8)$$

$$\varphi_{i3} = \varphi_{f3}[((r_3 + r_{i3})/r_3)^2 - 1]. \quad (9)$$

Therefore, all α parameters in Eqs. (2)–(4) can be related to φ_i as

$$\alpha = \sqrt{\varphi_i + \varphi_f}. \quad (10)$$

As a result, Ji model for all nanocomposites is given by φ_i as

$$E_c = E_m[1 - \sqrt{\varphi_i + \varphi_f}$$
$$+ \frac{\sqrt{\varphi_i + \varphi_f} - \sqrt{\varphi_f}}{1 - \sqrt{\varphi_i + \varphi_f} + \sqrt{\varphi_i + \varphi_f}(k-1)/\ln k}$$
$$+ \sqrt{\varphi}(1 - \sqrt{\varphi_i + \varphi_f} + 1/2(\sqrt{\varphi_i + \varphi_f}$$
$$- \sqrt{\varphi_f})(k+1) + \sqrt{\varphi_f} E_f/E_m)^{-1}]^{-1}. \quad (11)$$

According to Eqs. (7)–(9), φ_f can be expressed as a function of φ_i as

$$\varphi_{f1} = \frac{\varphi_{i1} t}{2t_i}, \quad (12)$$

$$\varphi_{f2} = \frac{\varphi_{i2}}{((r_2 + r_{i2})/r_2)^3 - 1}, \quad (13)$$

$$\varphi_{f3} = \frac{\varphi_{i3}}{((r_3 + r_{i3})/r_3)^2 - 1}. \quad (14)$$

Accordingly, Ji model can be defined by the properties of interphase for polymer nanocomposites containing different nanoparticles as

$$E = E_m[1 - \sqrt{\varphi_{i1} + \varphi_{i1}t/(2t_i)}$$
$$+ (\sqrt{\varphi_{i1} + \varphi_{i1}t/(2t_i)} - \sqrt{\varphi_{i1}t/(2t_i)})$$
$$\times (1 - \sqrt{\varphi_{i1} + \varphi_{i1}t/(2t_i)}$$
$$+ \sqrt{\varphi_{i1} + \varphi_{i1}t/(2t_i)}(k-1)/\ln k)^{-1}$$
$$+ (\sqrt{\varphi_{i1}t/(2t_i)}(1 - \sqrt{\varphi_{i1} + \varphi_{i1}t/(2t_i)}$$
$$+ 1/2(\sqrt{\varphi_{i1} + \varphi_{i1}t/(2t_i)}$$
$$- \sqrt{\varphi_{i1}t/(2t_i)})(k+1)$$
$$+ \sqrt{\varphi_{i1}t/(2t_i)} E_f/E_m)^{-1}]^{-1}, \quad (15)$$

$$E = E_m[(1 - \sqrt{\varphi_{i2} + \varphi_{i2}((r_2 + r_{i2})^3/r_2^3 - 1)^{-1}}$$
$$+ (\sqrt{\varphi_{i2} + \varphi_{i2}((r_2 + r_{i2})^3/r_2^3 - 1)^{-1}}$$
$$- \sqrt{\varphi_{i2}((r_2 + r_{i2})^3/r_2^3 - 1)^{-1}})$$
$$\times (1 - \sqrt{\varphi_{i2} + \varphi_{i2}((r_2 + r_{i2})^3/r_2^3 - 1)^{-1}}$$
$$+ \sqrt{\varphi_{i2} + \varphi_{i2}((r_2 + r_{i2})^3/r_2^3 - 1)^{-1}}$$
$$\times (k-1)\ln^{-1}k)^{-1}$$
$$+ \sqrt{\varphi_{i2}((r_2 + r_{i2})^3/r_2^3 - 1)^{-1}}$$
$$\times (1 - \sqrt{\varphi_{i2} + \varphi_{i2}((r_2 + r_{i2})^3/r_2^3 - 1)^{-1}}$$
$$+ 1/2(\sqrt{\varphi_{i2} + \varphi_{i2}((r_2 + r_{i2})^3/r_2^3 - 1)^{-1}}$$
$$- \sqrt{\varphi_{i2}((r_2 + r_{i2})^3/r_2^3 - 1)^{-1}})(k+1)$$
$$+ \sqrt{\varphi_{i2}((r_2 + r_{i2})^3/r_2^3 - 1)^{-1}} E_f/E_m)^{-1}]^{-1}, \quad (16)$$

$$E = E_m[(1 - \sqrt{\varphi_{i3} + \varphi_{i3}((r_3 + r_{i3})^2/r_3^2 - 1)^{-1}}$$
$$+ (\sqrt{\varphi_{i3} + \varphi_{i3}((r_3 + r_{i3})^2/r_3^2 - 1)^{-1}}$$
$$- \sqrt{\varphi_{i3}((r_3 + r_{i3})^2/r_3^2 - 1)^{-1}})$$
$$\times ((1 - \sqrt{\varphi_{i3} + \varphi_{i3}((r_3 + r_{i3})^2/r_3^2 - 1)^{-1}}$$
$$+ \sqrt{\varphi_{i3} + \varphi_{i3}((r_3 + r_{i3})^2/r_3^2 - 1)^{-1}}$$
$$\times (k-1)\ln^{-1}k)^{-1}$$
$$+ \sqrt{\varphi_{i3}((r_3 + r_{i3})^2/r_3^2 - 1)^{-1}}$$

$$\times (1 - \sqrt{\varphi_{i3} + \varphi_{i3}((r_3 + r_{i3})^2 / r_3^2 - 1)^{-1}}$$

$$+ 1/2 (\sqrt{\varphi_{i3} + \varphi_{i3}((r_3 + r_{i3})^2 / r_3^2 - 1)^{-1}}$$

$$- \sqrt{\varphi_{i3}((r_3 + r_{i3})^2 / r_3^2 - 1)^{-1}} (k+1))$$

$$+ \sqrt{\varphi_{i3}((r_3 + r_{i3})^2 / r_3^2 - 1)^{-1}} E_f / E_m)^{-1}]^{-1}, \quad (17)$$

which display the effects of interphase properties on the Young's modulus of polymer nanocomposites.

Pukanszky [18] suggested an equation based on the formation of interphase in composites, where the yield strength is determined as a function of filler content. Pukanszky model is presented as

$$\sigma_r = \frac{1 - \varphi_f}{1 + 2.5\varphi_f} \exp(B\varphi_f), \quad (18)$$

where σ_r is relative yield strength as σ_c / σ_m, σ_c and σ_m are yield strengths of composite and matrix, respectively, B is an interfacial parameter which assumes the capability of stress transfer between matrix and filler. This model was well applied for different polymer nanocomposites in the recent studies [19, 20]. Therefore, it is applied in this work to analyze the effects of interphase on yield strength of dissimilar nanocomposites. Parameter B depends to interphase characteristics as

$$B = (1 + A_c \rho_f r_i) \ln \left(\frac{\sigma_i}{\sigma_m} \right), \quad (19)$$

where A_c is the specific surface area of filler, ρ_f is density of filler, and σ_i is the tensile strength of interphase. To calculate parameter B, Pukanszky model can be rewritten as

$$\ln \left(\sigma_r \frac{1 + 2.5\varphi_f}{1 - \varphi_f} \right) = B\varphi_f, \quad (20)$$

where the linear plot of $\ln(\sigma_r(1 + 2.5\varphi_f)/(1 - \varphi_f))$ against φ_f shows the slope of B. Using Eqs. (12)–(14), Pukanszky model can be expressed as a function of interphase properties for polymer nanocomposites as

$$\sigma_{r1} = \frac{1 - t\varphi_{i1}/(2t_i)}{1 + 2.5 t\varphi_{i1}/(2t_i)} \exp(B_1 t\varphi_{i1}/(2t_i)), \quad (21)$$

$$\sigma_{r2} = \frac{1 - \varphi_{i2}((r_2 + r_{i2})^3 / r_2^3 - 1)^{-1}}{1 + 2.5\varphi_{i2}((r_2 + r_{i2})^3 / r_2^3 - 1)^{-1}}$$

$$\times \exp[B_2 \varphi_{i2}((r_2 + r_{i2})^3 / r_2^3 - 1)^{-1}], \quad (22)$$

$$\sigma_{r3} = \frac{(r_3 + r_{i3})^2 / r_3^2 - 1 - \varphi_{i3}}{(r_3 + r_{i3})^2 / r_3^2 - 1 + 2.5\varphi_{i3}}$$

$$\times \exp[B_3 \varphi_{i3}((r_3 + r_{i3})^2 / r_3^2 - 1)^{-1}]. \quad (23)$$

Additionally, A_c can be defined for layered, spherical and cylindrical nanoparticles as

$$A_{c1} = \frac{A_1}{m_1} = \frac{A_1}{\rho_{f1}v_1} \cong \frac{2l^2}{\rho_{f1}l^2 t} = \frac{2}{\rho_{f1}t}, \quad (24)$$

$$A_{c2} = \frac{A_2}{m_2} = \frac{A_2}{\rho_{f2}v_2} = \frac{4\pi r_2^2}{\rho_{f2}4/3\pi r_2^3} = \frac{3}{\rho_{f2}r_2}, \quad (25)$$

$$A_{c3} = \frac{A_3}{m_3} = \frac{A_3}{\rho_{f3}v_3} = \frac{2\pi r_3 l}{\rho_{f3}\pi r_3^2 l} = \frac{2}{\rho_{f3}r_3}, \quad (26)$$

where A, m, v and l are the surface area, mass, volume and length of nanoparticles, respectively. As a result, B can be expressed for polymer nanocomposites as

$$B_1 = \left(1 + \frac{\varphi_{i1}}{\varphi_{f1}} \right) \ln \frac{\sigma_{i1}}{\sigma_m}, \quad (27)$$

$$B_2 = \left[3 \left(\frac{\varphi_{i2}}{\varphi_{f2}} + 1 \right)^{1/3} - 2 \right] \ln \frac{\sigma_{i2}}{\sigma_m}, \quad (28)$$

$$B_3 = \left[2 \left(\frac{\varphi_{i3}}{\varphi_{f3}} + 1 \right)^{1/2} - 1 \right] \ln \frac{\sigma_{i3}}{\sigma_m}. \quad (29)$$

3. RESULTS AND DISCUSSION

3.1. The Analysis of Experimental Data from the Literature

In this section, the mentioned models are utilized to determine the properties of interphase in several samples from the literature. In addition, the effects of interphase characteristics on the modulus and strength of polymer nanocomposites are plotted. Table 1 shows different samples from the literature as well as the properties of neat polymer and nanofiller. The experimental tensile moduli of samples are applied to Ji model (Eqs. (1)–(6)) and the average levels of t_i or r_i and E_i are calculated. The interphase thickness cannot be more than the gyration radius of polymer chains and E_i changes between the moduli of polymer matrix and nanofiller. Therefore, suitable r_i or t_i and E_i are chosen from the explained ranges and finally, the average values of interphase properties are given in Table 1. The presented data show the significant thickness of interphase in the reported samples. Additionally, a high interphase modulus is calculated in all reported samples, which is more than the stiffness of polymer matrix. Accordingly, the interphase can play an important role in the performances of polymer nanocomposites.

Moreover, the experimental yield strength of samples is fitted to Pukanszky model (Eq. (18)) to determine the B parameter. Parameter B is applied into Eq. (19) to measure σ_i values. Table 1 gives the values

Table 1. The samples and calculated interphase properties

No.	Sample	r or t, nm	ρ_f, g cm^{-3}	E_m, GPa	σ_m, MPa	r_i or t_i, nm Eqs. (2)–(4)	E_i, GPa Eqs. (1)–(6)	B Eq. (20)	σ_i, MPa Eq. (19)	A_c, m^2 g^{-1} Eqs. (24)–(26)
1	PBT[1]/nanoclay [21]	2	1.98	2.14	55.2	12.0	9.60	4.83	80.0	505.1
2	PA11[2]/nanoclay [22]	4	1.90	0.61	32.8	12.0	2.50	8.40	108.9	526.3
3	LLDPE[3]/SiO$_2$ [23]	8	2.20	3.70	51.0	12.0	11.10	24.60	4467.0	170.5
4	Epoxy/MWCNT[4] [24]	15	1.90	1.90	45.0	22.5	133.00	7.66	305.4	70.2
5	PEI[5]/MWCNT [25]	9	2.10	2.96	102.0	11.0	8.80	5.94	573.5	117.0

1—poly(butylene terephthalate), 2—polyamide 11, 3—linear low density polyethylene, 4—multiwalled carbon nanotubes, 5—polyetherimide.

of B and σ_i data. The diverse B data show the dissimilar levels of interfacial adhesion in the samples. Additionally, different σ_i data are obtained for reported samples. The highest σ_i is obtained for sample No. 3 as 4467 MPa and the least level is found for sample No. 1 as 80 MPa. The σ_i results are much higher than σ_m demonstrating the significant strength of formed interphase in the reported samples.

The dimension and level of interphase are attributed to some parameters such as interfacial area and compatibility between polymer matrix and nanofiller which control the interfacial interaction. Some procedures such as treatment, modification and functionalization of nanofillers can encourage the compatibility and interfacial adhesion between the components of nanocomposites. Furthermore, A_c data are reported in Table 1 using Eqs. (24)–(26). The nanoclay produces the highest level of A_c among the nanoparticles. This occurrence causes the highest level of interfacial area between polymer matrix and nanoclay layers, which finally creates the highest level of reinforcement in polymer nanocomposite. In fact, the high value of A_c is the significant advantage of nanofiller, which makes the unexpected behavior in polymer nanocomposites. According to Eqs. (24)–(26), A_c is inversely related to r and t and the smallest nanoparticles create the highest level of A_c as shown in Table 1.

Figure 1 illustrates the volume fraction φ_i in some reported samples by Eqs. (7)–(9). It is observed that the interphase occupies a large volume in polymer nanocomposites which is more than the nanofiller volume in some samples. Volume fraction φ_i increases with nanofiller content in all samples. The high level of interphase confirms the significant influence of this phase beside matrix and nanofiller phases. As a result, assuming the interphase is compulsory for estimation of mechanical properties in polymer nanocomposites. In addition, φ_i is directly related to the thickness of interphase (according to Eqs. (7)–(9)), i.e. φ_i increases when the thickness of interphase enlarges.

3.2. The Roles of Interphase Properties According to the Models

Figure 2 demonstrates the effects of φ_i and E_i on modulus of polymer nanocomposites containing spherical nanoparticles by Eq. (16). The Young's modulus more depends to φ_i than E_i.
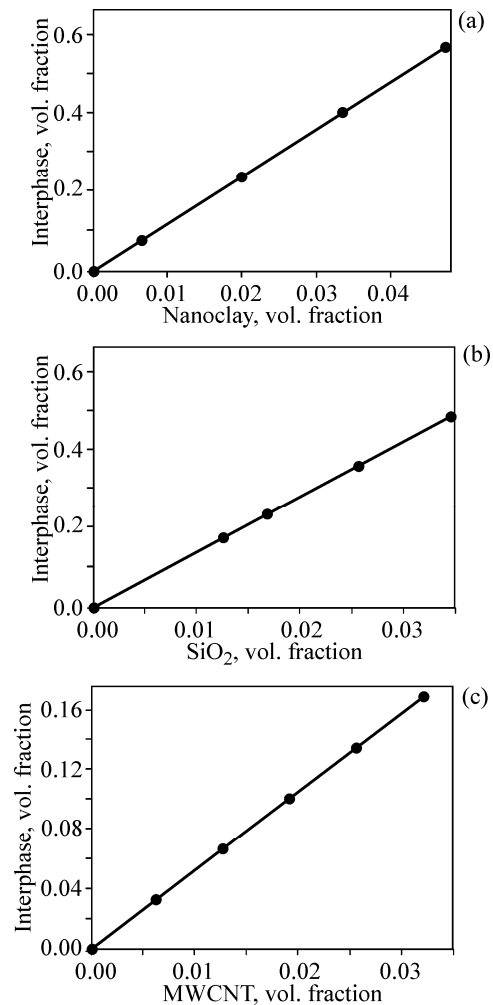

Fig. 1. φ_i as a function of φ_f in PBT/nanoclay [21] (No. 1) (a), LLDPE/SiO$_2$ [23] (No. 3) (b) and epoxy/MWCNT [24] (No. 4) samples (c).
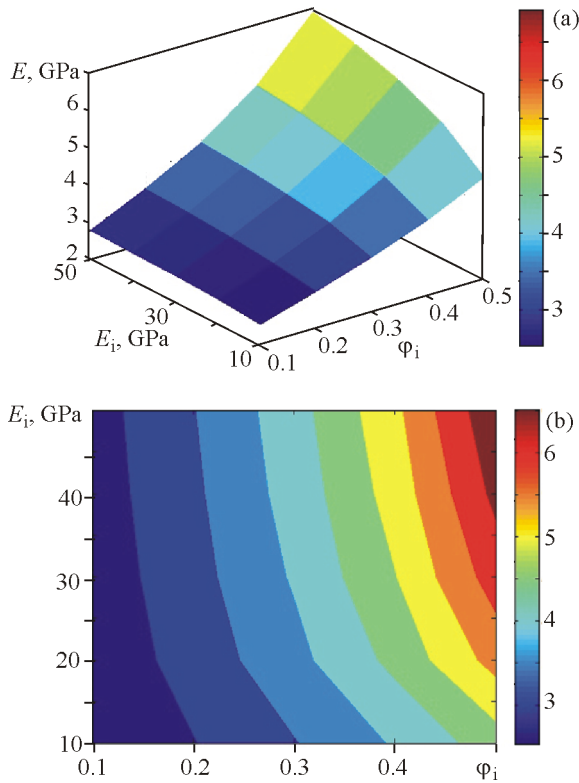
Fig. 2. Roles of φ_i and E_i in the Young's modulus of polymer nanocomposites containing spherical nanoparticles by Eq. (16) in $r_2 = 15$ nm, $r_{i2} = 10$ nm and $E_m = 2$ GPa: (a) 3D and (b) contour plots (color online).
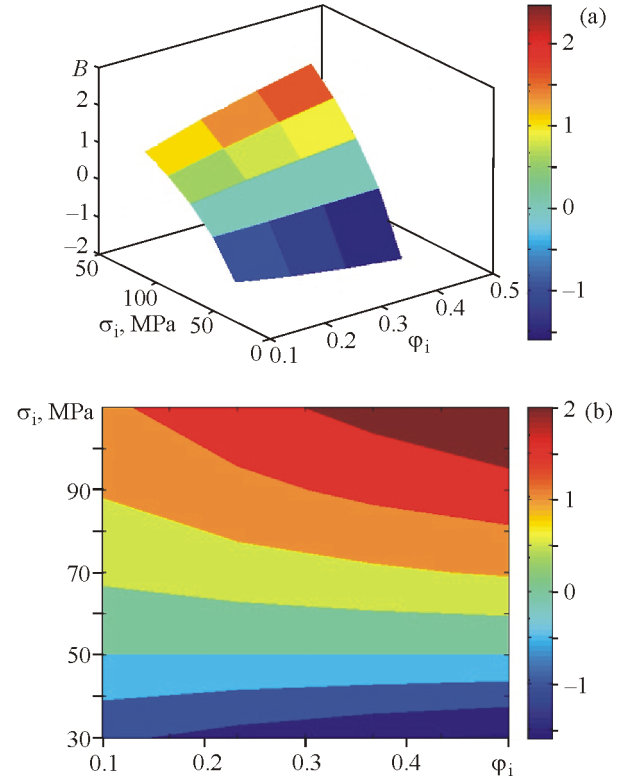
Fig. 3. 3D (a) and contour plots (b) to show the effects of φ_i and σ_i on parameter B in polymer nanocomposites containing spherical nanoparticles (Eq. (28)) in $\varphi_{f3} = 0.1$ and $\sigma_m = 50$ MPa (color online).

The low φ_i generally results in a low modulus at all E_i levels. However, the best modulus is obtained by high levels of φ_i and E_i. It means that φ_i and E_i have optimistic effects on the modulus of nanocomposites, where the effect of E_i becomes important at high values of φ_i indicating the important role of φ_i in Young's modulus of polymer nanocomposites.

Figure 3 exhibits the influences of φ_i and σ_i on parameter B in polymer nanocomposites containing spherical nanoparticles (Eq. (28)). Parameter B shows comparatively same levels at all φ_i values depended to the level of σ_i. In other words, σ_i more expressively affects the level of parameter B compared with φ_i.

Parameter B shows negative values when σ_i is lower than σ_m at all φ_i. The best level of B is obtained in the highest values of φ_i and σ_i. As a result, B is more depended to σ_i value in polymer nanocomposites (especially at low σ_i), while formation of a high-volume interphase improves the magnitude of B interfacial parameter.

Figure 4 also shows the roles of nanoparticle radius and interphase thickness on the interphase fraction φ_{i2} of nanocomposites containing spherical nanoparticles

by Eq. (8) in $\varphi_{i2} = 0.02$. The high values of nanoparticle size decrease the φ_{i2}, but the small radius of nanoparticles increases it. On the other hand, a thick interphase grows the level of φ_{i2}, while the thinner one produces a smaller φ_{i2}. Therefore, small nanoparticles and thick interphase show beneficial effects on the φ_{i2}.

Since a higher volume fraction of interphase causes a better level for tensile modulus and strength (Figs. 2 and 3), it is concluded that small particles and thick interphase introduce the high mechanical properties in nanocomposites. Likewise, large particles and thin interphase result in low levels for mechanical performances. The small nanoparticles induce the high specific surface area between polymer and nanoparticles. A good interphase is gained by the high level of interfacial interaction/adhesion in nanocomposites [20, 26].

A micromechanical model was also proposed by Boutaleb et al. [27] to calculate the modulus and yield stress in polymer/SiO$_2$ nanocomposites. It considers the interphase as the perturbed region of polymer matrix around the nanoparticles. The predicted effects of nanoparticle radius, interphase thickness and modulus
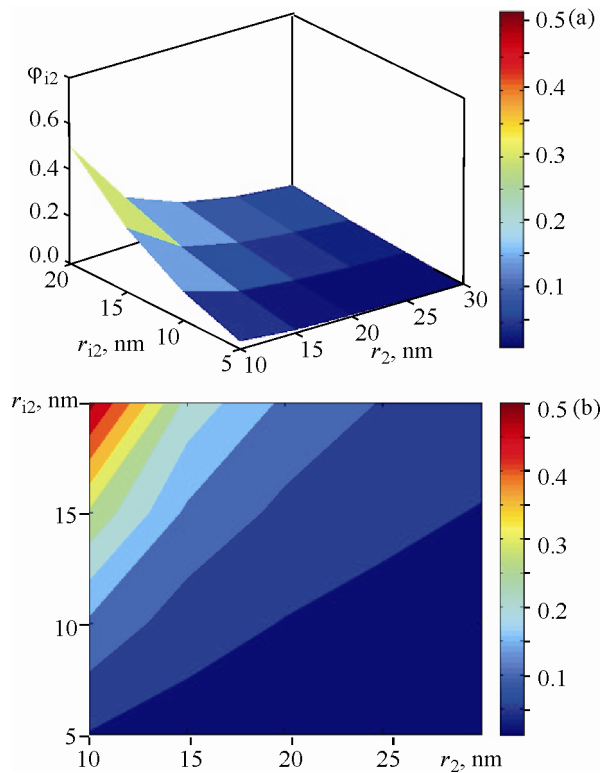
Fig. 4. Volume fraction φ_{i2} as a function of r_2 and r_{i2} (Eq. (8)) in $\varphi_{f2} = 0.02$: 3D (a) and contour plots (b) (color online).

on the modulus and yield strength of nanocomposites in that work are similar to those suggested in the present study. All these remarks confirm the progressive roles of interphase properties in the mechanical behavior of nanocomposites.

4. CONCLUSIONS

Ji and Pukanszky models were used to show the Young's modulus and yield strength of different polymer nanocomposites as a function of interphase volume fraction, thickness, modulus and strength. The interphase properties of different samples were also studied based on Young's modulus and yield strength. The Young's modulus more depends on φ_f and φ_i than E_i. A low φ_i generally results in a low modulus at all E_i values. The poorest Young's modulus is found by the thinnest interphase. Besides, small nanoparticles and thick interphase increase the yield strength of nanocomposites. Parameter σ_i more expressively affects the level of parameter B compared to φ_i. Nevertheless, the highest values of φ_i and σ_i produce the highest level of interfacial adhesion expressed by parameter B. Since a high level of B increases the yield strength of

nanocomposites, the high values of φ_i and σ_i play positive roles in the yield strength.

REFERENCES

1. Zare, Y. and Rhee, K.Y., Evaluation and Development of Expanded Equations Based on Takayanagi Model for Tensile Modulus of Polymer Nanocomposites Assuming the Formation of Percolating Networks, *Phys. Mesomech.*, 2018, vol. 21, no. 4, pp. 351–357.
2. Panin, V.E., Surikova, N.S., Smirnova, A.S., and Pochivalov, Yu.I., Mesoscopic Structural States in Plastically Deformed Nanostructured Metal Materials, *Phys. Mesomech.*, 2018, vol. 21, no. 5, pp. 396–400. doi 10.1134/S102995991805003X
3. Nikonov, A.Yu., Zharmukhambetova, A.M., Ponomareva, A.V., and Dmitriev, A.I., Numerical Study of Mechanical Properties of Nanoparticles of β-Type Ti-Nb Alloy under Conditions Identical to Laser Sintering. Multilevel Approach, *Phys. Mesomech.*, 2018, vol. 21, no. 1, pp. 43–51.
4. Badamshina, E.R., Goldstein, R.V., Ustinov, K.B., and Estrin, Ya.I., Strength and Fracture Toughness of Polyurethane Elastomers Modified with Carbon Nanotubes, *Phys. Mesomech.*, 2018, vol. 21, no. 3, pp. 187–192.
5. Mauroy, H., Plivelic, T.S., Suuronen, J.-P., Hage, F.S., Fossum, J.O., and Knudsen, K.D., Anisotropic Clay–Polystyrene Nanocomposites: Synthesis, Characterization and Mechanical Properties, *Appl. Clay Sci.*, vol. 108, pp. 19–27.
6. Boumbimba, R.M., Wang, K., Bahlouli, N., Ahzi, S., Rémond, Y., and Addiego, F., Experimental Investigation and Micromechanical Modeling of High Strain Rate Compressive Yield Stress of a Melt Mixing Polypropylene Organoclay Nanocomposites, *Mech. Mater.*, 2012, vol. 52, pp. 58–68.
7. Miyagawa, H., Rich, M.J., and Drzal, L.T., Amine-Cured Epoxy/Clay Nanocomposites. II. The Effect of the Nanoclay Aspect Ratio, *J. Polym. Sci. B. Polym. Phys.*, 2004, vol. 42, pp. 4391–4400.
8. Odegard, G., Clancy, T., and Gates, T., Modeling of the Mechanical Properties of Nanoparticle/Polymer Composites, *Polymer*, 2005, vol. 46, pp. 553–562.
9. Pontefisso, A., Zappalorto, M., and Quaresimin, M., An Efficient RVE Formulation for the Analysis of the Elastic Properties of Spherical Nanoparticle Reinforced Polymers, *Comput. Mater. Sci.*, 2015, vol. 96, pp. 319–326.
10. Hassanzadeh-Aghdam, M.K., Ansari, R., and Mahmoodi, M.J., Thermo-Mechanical Properties of Shape Memory Polymer Nanocomposites Reinforced by Carbon Nanotubes, *Mech. Mater.*, 2019, vol. 129, pp. 80–98.
11. Ishak, Z.M., Chow, W., and Takeichi, T., Compatibilizing Effect of SEBS-g-MA on the Mechanical Properties of Different Types of OMMT Filled Polyamide

6/Polypropylene Nanocomposites, *Compos. A. Appl. Sci. Manufact.*, 2008, vol. 39, pp. 1802–1814.

12. Zare, Y. and Rhee, K.Y., Tensile Strength Prediction of Carbon Nanotube Reinforced Composites by Expansion of Cross-Orthogonal Skeleton Structure, *Compos. B. Eng.*, 2019, vol. 161, pp. 601–607.

13. Zare, Y. and Rhee, K.Y., Evaluation of the Tensile Strength in Carbon Nanotube-Reinforced Nanocomposites Using the Expanded Takayanagi Model, *JOM*, 2019, pp. 1–9.

14. Zare, Y., Modeling Approach for Tensile Strength of Interphase Layers in Polymer Nanocomposites, *J. Coll. Int. Sci.*, 2016, vol. 471, pp. 89–93.

15. Lu, P., Leong, Y., Pallathadka, P., and He, C., Effective Moduli of Nanoparticle Reinforced Composites Considering Interphase Effect by Extended Double-Inclusion Model—Theory and Explicit Expressions, *Int. J. Eng. Sci.*, 2013, vol. 73, pp. 33–55.

16. Zare, Y., Determination of Polymer–Nanoparticles Interfacial Adhesion and Its Role in Shape Memory Behavior of Shape Memory Polymer Nanocomposites, *Int. J. Adhes. Adhesiv.*, 2014, vol. 54, pp. 67–71.

17. Ji, X.L., Jing, J.K., Jiang, W., and Jiang, B.Z., Tensile Modulus of Polymer Nanocomposites, *Polymer Eng. Sci.*, 2002, vol. 42, pp. 983–993.

18. Pukanszky, B., Influence of Interface Interaction on the Ultimate Tensile Properties of Polymer Composites, *Composites*, 1990, vol. 21, pp. 255–262.

19. Szazdi, L., Pozsgay, A., and Pukanszky, B., Factors and Processes Influencing the Reinforcing Effect of Layered Silicates in Polymer Nanocomposites, *Eur. Polymer J.*, 2007, vol. 43, pp. 345–359.

20. Dominkovics, Z., Hári, J., Kovács, J., Fekete, E., and Pukánszky, B., Estimation of Interphase Thickness and Properties in PP/Layered Silicate Nanocomposites, *Eur. Polymer J.*, 2011, vol. 47, pp. 1765–1774.

21. Chang, Y.W., Kim, S., and Kyung, Y., Poly (Butylene Terephthalate)–Clay Nanocomposites Prepared by Melt Intercalation: Morphology and Thermomechanical Properties, *Polymer Int.*, 2005, vol. 54, pp. 348–353.

22. Hu, Y., Shen, L., Yang, H., Wang, M., Liu, T., Liang, T., and Zhang, J., Nanoindentation Studies on Nylon 11/Clay Nanocomposites, *Polym. Test*, 2006, vol. 25, pp. 492–497.

23. Kontou, E. and Niaounakis, M., Thermo-Mechanical Properties of LLDPE/SiO$_2$ Nanocomposites, *Polymer*, 2006, vol. 47, pp. 1267–1280.

24. Yeh, M.-K., Hsieh, T.-H., and Tai, N.-H., Fabrication and Mechanical Properties of Multi-Walled Carbon Nanotubes/Epoxy Nanocomposites, *Mater. Sci. Eng. A*, 2008, vol. 483, pp. 289–292.

25. Isayev, A., Kumar, R., and Lewis, T.M., Ultrasound Assisted Twin Screw Extrusion of Polymer–Nanocomposites Containing Carbon Nanotubes, *Polymer*, 2009, vol. 50, pp. 250–260.

26. Li, Y., Waas, A.M., and Arruda, E.M., The Effects of the Interphase and Strain Gradients on the Elasticity of Layer by Layer (LBL) Polymer/Clay Nanocomposites, *Int. J. Solid. Struct.*, 2011, vol. 48, pp. 1044–1053.

27. Boutaleb, S., Zanri, F., Mesbah, A., Naıt-Abdelaziz, M., Gloaguen, J.-M., Boukharouba, T., and Lefebvre, J.-M., Micromechanics-Based Modelling of Stiffness and Yield Stress for Silica/Polymer Nanocomposites, *Int. J. Solid. Struct.*, 2009, vol. 46, pp. 1716–1726.